Article:
Li, K, Zou, H, Ettelaie, R orcid.org/0000-0002-6970-4650 et al. (2 more authors) (Cover date: April 3, 2023) Spatial Localization of Two Enzymes at Pickering Emulsion Droplet Interfaces for Cascade Reactions. Angewandte Chemie International Edition, 62 (15). e202300794. ISSN 1433-7851

https://doi.org/10.1002/anie.202300794

Supporting Information

CO_2-switchable thermoresponsiveness of poly(*N*,*N*-(diethylamino) ethyl acrylamide)-based homo- and copolymers in water

Fang Yin, Barbara Lonetti, Jean-Daniel Marty* and Nancy Lauth-de Viguerie*

Laboratoire des IMRCP, CNRS UMR 5623, Université de Toulouse, UPS, 118 route de Narbonne, F-31062 Toulouse, France.

*Corresponding authors:
N. Lauth-de Viguerie, E-mail: nancy.de-viguerie@univ-tlse3.fr
J.-D. Marty, E-mail: jean-daniel.marty@univ-tlse3.fr

1. Synthesis of *N*, *N*-(diethylamino) ethyl acrylamide monomer (DEAEAM)

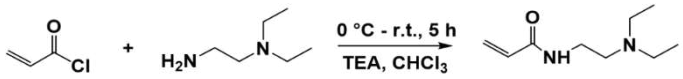

Scheme S1. Synthetic route for preparing DEAEAM monomer.

DEAEAM was prepared according to the previously described procedure. [1, 2] Briefly, *N*, *N*-diethylethylenediamine (60 mmol, 6.972 g), triethylamine (TEA, 72 mmol, 7.286 g) and $CHCl_3$ (100 mL) were added in a Schlenk flask under argon atmosphere in an ice-water bath. Acryloyl chloride (72 mmol, 6 mL) dissolved in $CHCl_3$ was added dropwise into flask within 1 h, after complete addition, the reaction was warmed up to room temperature for 4 h. Then the reaction mixture was washed with dilute NaOH solution and with deionized water three times, respectively. The organic phase was collected and concentrated under reduced pressure, the resulting residue was purified by aluminum oxide column chromatography (petroleum ether/ethyl acetate gradient 3:1 to 0:1, v/v) to give DEAEAM (5.39 g, yield: 53%). ^{1}H NMR (300 MHz, $CDCl_3$) δ_H (ppm): 6.43 (s, 1H, -N<u>H</u>-), 6.21 (dd, 1H, C<u>H</u>$_2$=CH-), 6.08 (dd, 1H, C<u>H</u>$_2$=CH-), 5.55 (dd, 1H, CH$_2$=C<u>H</u>-), 3.32 (q, 2H, -NH-C<u>H</u>$_2$-), 2.55-2.44 (m, 6H, -N(C<u>H</u>$_2$)$_3$), 0.96 (t, 6H, -C<u>H</u>$_3$) ; ^{13}C NMR (75 MHz, $CDCl_3$) δ_C (ppm): 165.51, 131.13, 125.78, 51.28, 46.68, 36.90 and 11.75 (**Figures S1** and **S2**)

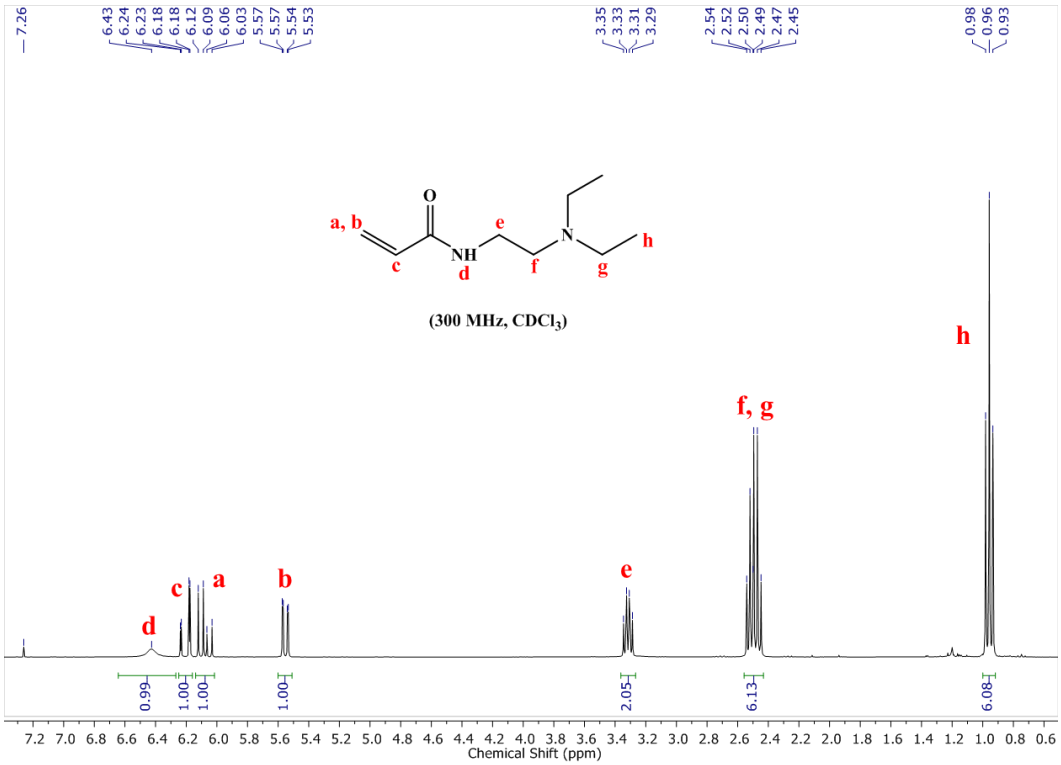

Figure S1. ^{1}H NMR spectrum of DEAEAM in $CDCl_3$.

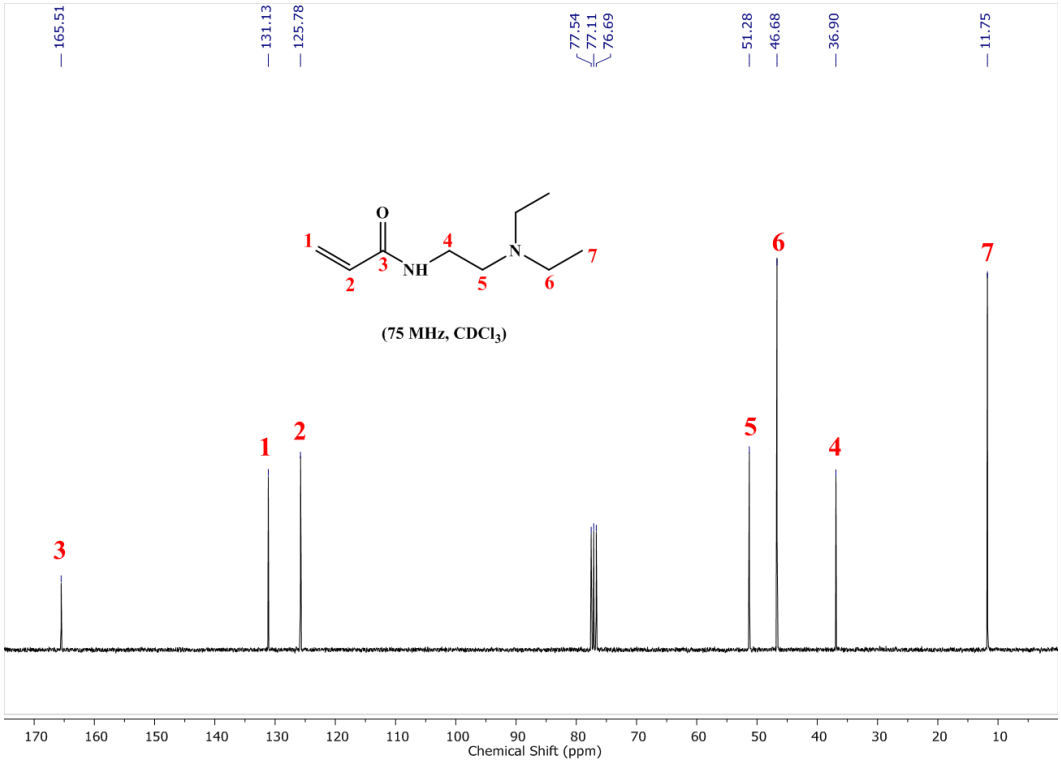

Figure S2. ^{13}C NMR spectrum of DEAEAM in $CDCl_3$.

2. Synthesis of homopolymer and block copolymer

PDEAEAM-based homopolymer and block copolymers were synthesized by reversible addition-fragmentation chain-transfer (RAFT) polymerization as follows.

2.1. Synthesis of poly(*N*,*N*-(diethylamino) ethyl acrylamide) (PD_{5K})

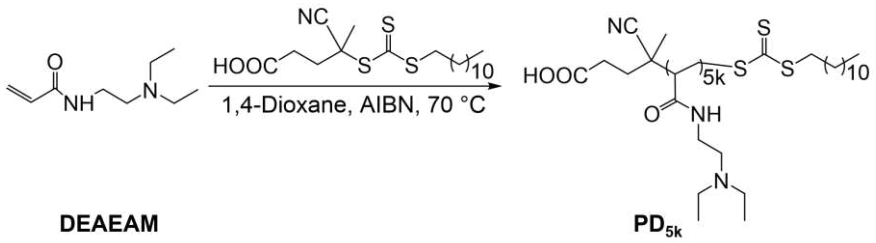

Scheme S2. Synthetic route for preparing PD_{5k} via RAFT polymerization.

A typical reaction was as follows: A Schlenk tube was charged with DEAEAM (2 g, 11.747 mmol), AIBN (0.050 g, 0.305 mmol), CDTPA (0.176 g, 0.435 mmol), 1,3,5-trioxane (0.106 g, 1.175 mmol, as internal standard), 1,4-dioxane (3.497 g) and a stirring magnetic bar. The tube underwent freeze-vacuum-thaw for three cycles and then placed in an oil bath at 70 °C. After reaction for the given time, the resulting solution was immersed into liquid nitrogen to deactivate the free radicals. Then the product was purified by dialysis against deionized water for three days and dried by lyophilization. Conversion: 95.4%. $M_{n,theo}$ = 4790 g·mol^{-1}, $M_{n,NMR}$ = 4810 g·mol^{-1}. In DMF (containing 10 mM LiBr): $M_{n,SEC}$ = 6900 g·mol^{-1}, Đ = 1.21; in THF (containing 2 v% TEA): $M_{n,SEC}$ = 4210 g·mol^{-1}, Đ = 1.09. ^{1}H NMR (500 MHz, D_2O, 25 °C) δ_H (ppm): 3.33 (s, 2H, -CONH-C$\underline{H}_2$-), 2.64 (s, 6H, -N(C$\underline{H}_2$)$_3$), 2.31-1.62 (m, -C$\underline{H}_2$CH-CONH-, -CH$_2$C$\underline{H}$-CONH-, -C(CN)-C$\underline{H}_3$)-, -C$\underline{H}_2$CH$_2$COOH, -CH$_2$C$\underline{H}_2$COOH), 1.26 (s, 20H, -(C$\underline{H}_2$)$_{10}$-CH$_3$), 1.08 (s, 6H, -N(CH$_2$C$\underline{H}_3$)$_2$), 0.88 (t, 3H, -(CH$_2$)$_{10}$-C$\underline{H}_3$).

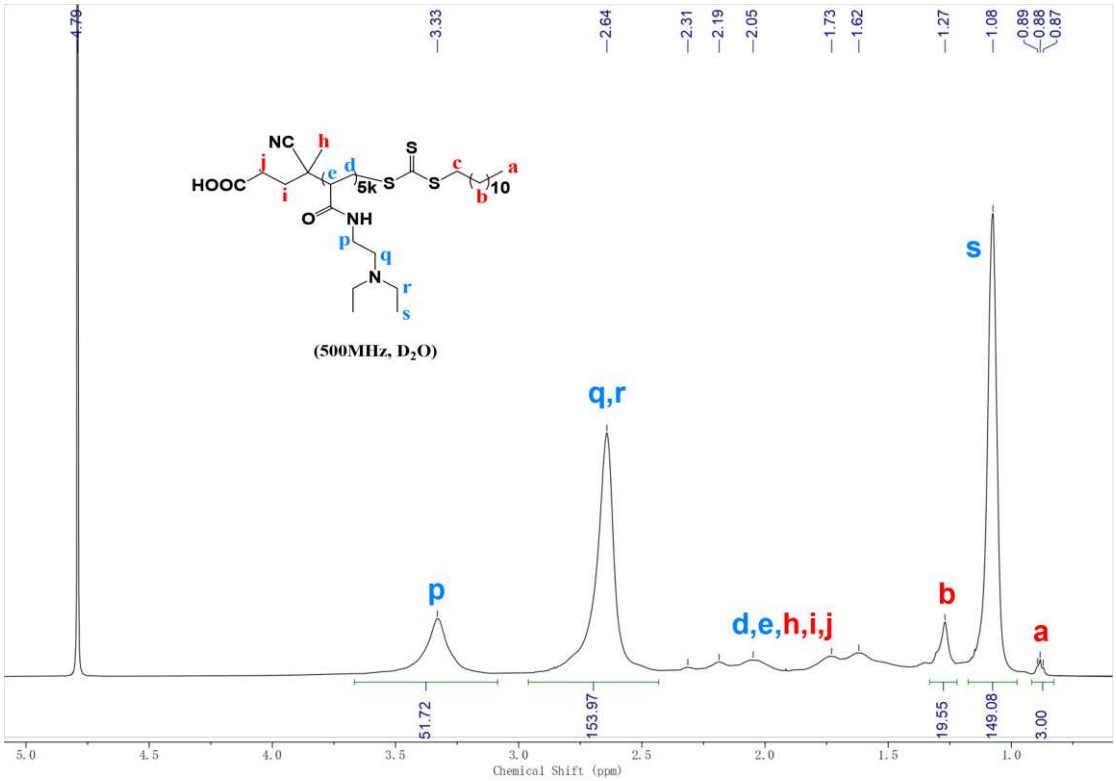

Figure S3. ^{1}H NMR spectrum of PD_{5k} in D_2O.

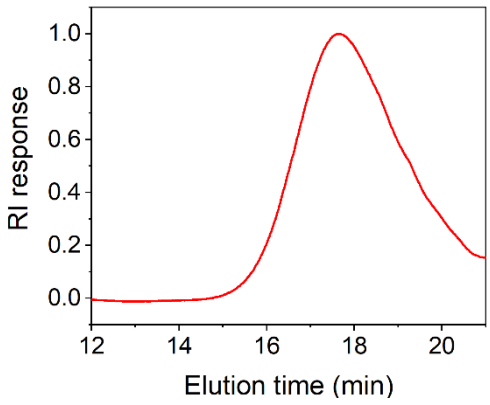

Figure S4. SEC trace of PD_{5k} in THF (containing 2 v% TEA).

2.2. Synthesis of poly(*N*-isopropylacrylamide)-*block*-poly(*N*,*N*-(diethylamino) ethyl acrylamide) (PN-*b*-PD)

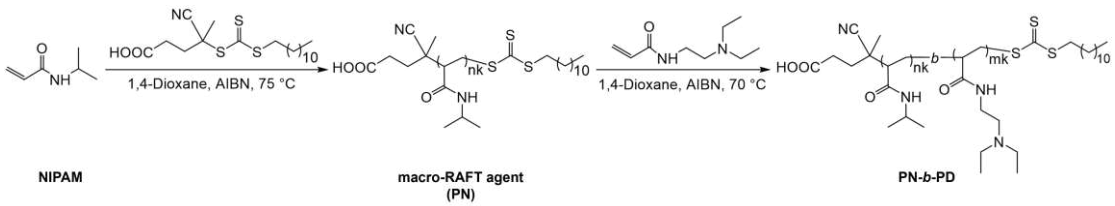

Scheme S3. Synthetic route for preparing PN-*b*-PD via RAFT polymerization.

2.2.1 Synthesis of poly(*N*-isopropylacrylamide) macro-RAFT agent (**PN_{5k}**)

A general synthetic procedure was as follows: NIPAM (2 g, 17.674 mmol), AIBN (0.036 g, 0.218 mmol), CDTPA (0.176 g, 0.436 mmol) and 1,4-dioxane (4.741 g) were added into a Schlenk flask, followed by three cycles of freeze-pump-thaw, then placed in a preheated oil bath at 75 °C. After a given time, the reaction was terminated by rapid immersion of tube in liquid nitrogen, the resulting mixture was concentrated and precipitated in cold diethyl ether twice to remove unreacted NIPAM, the purified product was dried under vacuum. Conversion: 99.9%. $M_{n,theo}$ = 5000 g·mol^{-1}, $M_{n,NMR}$ = 6130 g·mol^{-1}. In DMF (containing 10 mM LiBr): $M_{n,SEC}$ = 6080 g·mol^{-1}, Đ= 1.06; In THF (containing 2 v% TEA): $M_{n,SEC}$= 4720 g·mol^{-1}, Đ =1.03. ^{1}H NMR (500 MHz, D_2O, 25 °C) δH (ppm): 3.92 (s, 1H, -C<u>H</u>$(CH_3)_2$), 2.52-1.60 (m, C<u>H</u>$_2$CH-CONH-, -CH_2C<u>H</u>-CONH-, -C(CN)-C<u>H</u>$_3$)-, -C<u>H</u>$_2$$CH_2$COOH, -$CH_2$C<u>H</u>$_2$COOH), 1.33 (s, 20H, -(C<u>H</u>$_2$)$_{10}$-CH_3), 1.16 (s, 6H, -CH(C<u>H</u>$_3$)$_2$), 0.85 (s, 3H, -$(CH_2)_{10}$-C<u>H</u>$_3$).

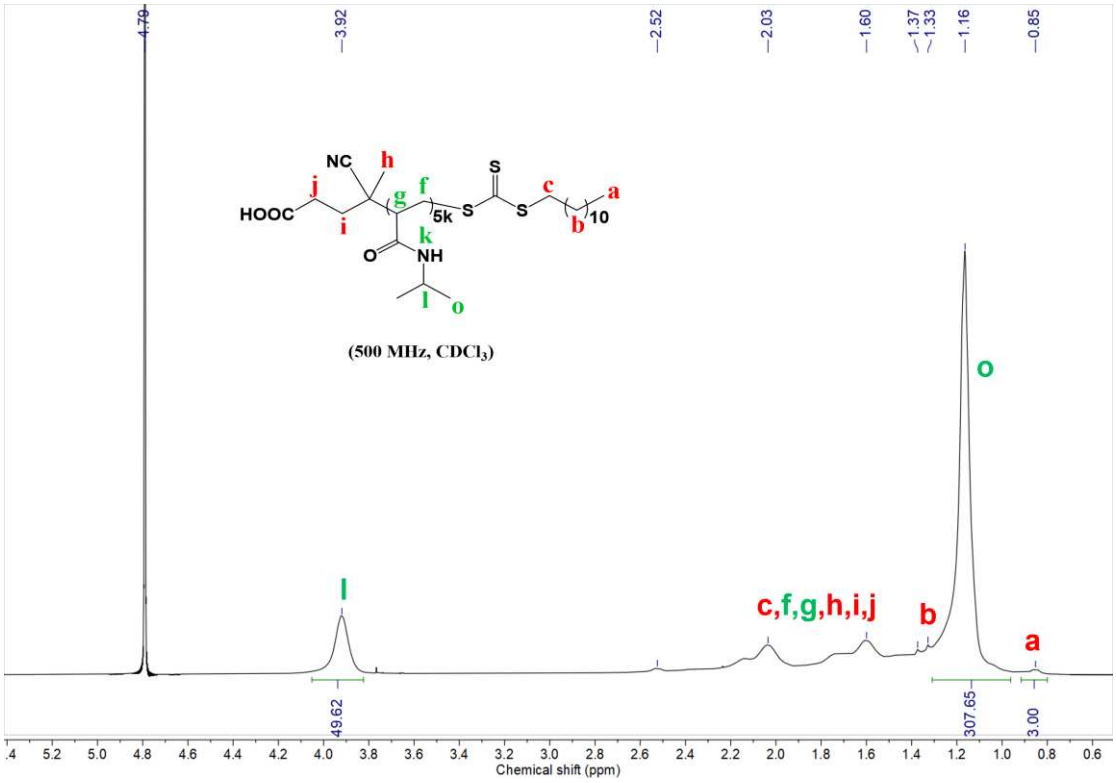

Figure S5. ^{1}H NMR spectrum of macro-RAFT agent PN_{5k} in D_2O.

2.2.2. Synthesis of poly(*N*-isopropylacrylamide)-*block*-poly(*N,N*-(diethylamino) ethyl acrylamide) (**PN_{5k}-*b*-PD_{5k}**)

A mixture of macro-RAFT agent PN_{5k} (2 g, 0.4 mmol), DEAEAM (2 g, 11.747 mmol), AIBN (0.059 g, 0.36 mmol), 1,3,5-trioxane (0.106 g, 1.175 mmol, as an internal standard) dissolving in 1,4-dioxane (3.43 g) was placed into a Schlenk flask with a magnetic stirrer. After three freeze-pump-thaw cycles, the tube was placed into a preheated oil bath at 70 °C. After a given time, the polymerization reaction was stopped by rapid cooling in liquid nitrogen. The purified product was precipitated in cold diethyl ether twice and dried under vacuum. Conversion:

96.6%. $M_{n,theo}$ = 9840 g·mol^{-1}. $M_{n,NMR}$ = 11090 g·mol^{-1}. In DMF (containing 10 mM LiBr): $M_{n,SEC}$ = 8340 g·mol^{-1}, Đ = 1.09; in THF (containing 2 v% TEA): $M_{n,SEC}$ = 6860 g·mol^{-1}, Đ = 1.16. ^{1}H NMR (500 MHz, D_2O, 25 ºC) δ_H (ppm): 3.90 (s, 1H, -C<u>H</u>$(CH_3)_2$), 3.32 (s, 2H, -CONH-C<u>H</u>$_2$-), 2.63 (s, 6H, -N(C<u>H</u>$_2)_3$), 2.02-1.33 (m, -C<u>H</u>$_2$CH-CONH-, -CH$_2$C<u>H</u>-CONH-, -C(CN)-C<u>H</u>$_3$)-, -C<u>H</u>$_2$CH$_2$COOH, -CH$_2$C<u>H</u>$_2$COOH), 1.25 (s, 20H, -(C<u>H</u>$_2)_{10}$-CH$_3$), 1.14 (s, 6H, -NHCH(C<u>H</u>$_3)_2$), 1.06 (s, 6H, -N(CH$_2$C<u>H</u>$_3)_2$), 0.86 (s, 3H, -(CH$_2)_{10}$-C<u>H</u>$_3$).

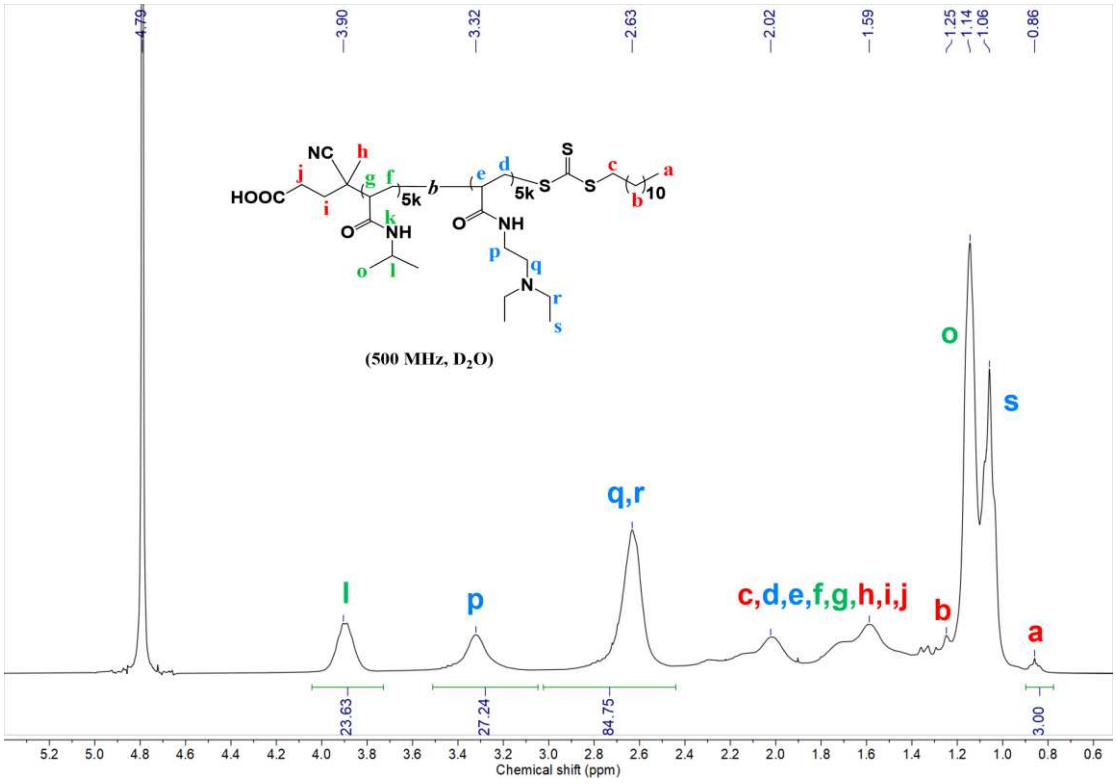

Figure S6. ^{1}H NMR spectrum of PN$_{5k}$-*b*-PD$_{5k}$ in D_2O.

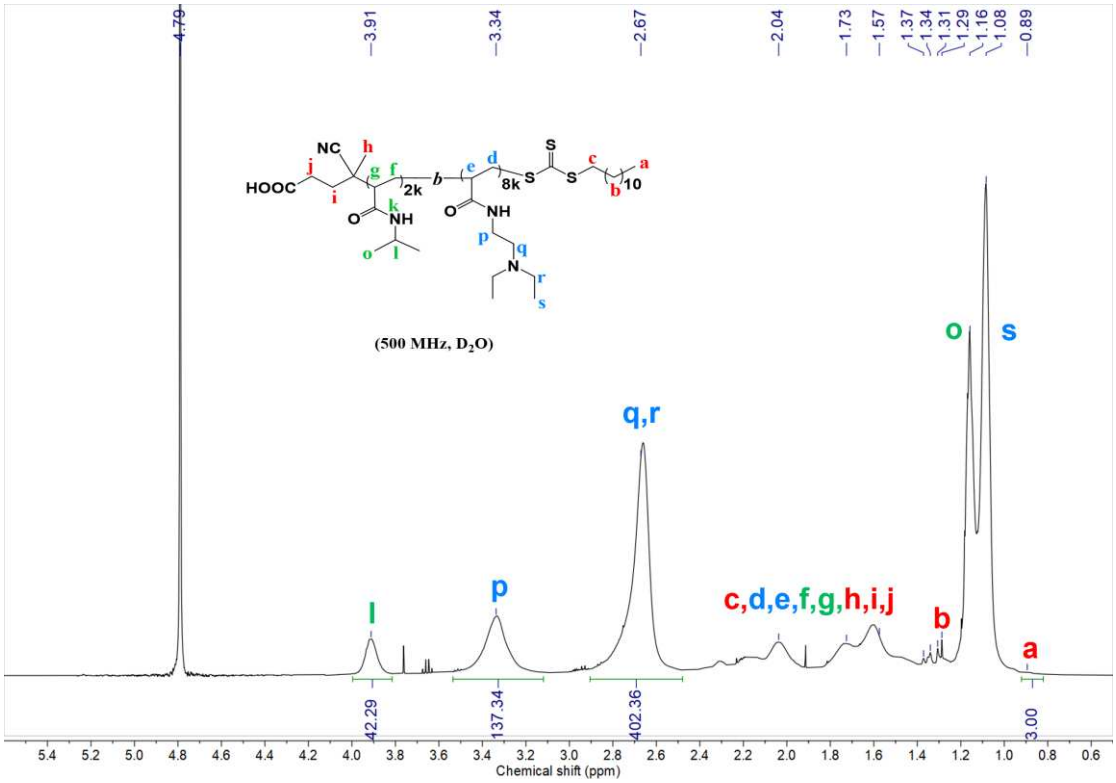

Figure S7. ^{1}H NMR spectrum of PN_{2k}-*b*-PD_{8k} in D_2O.

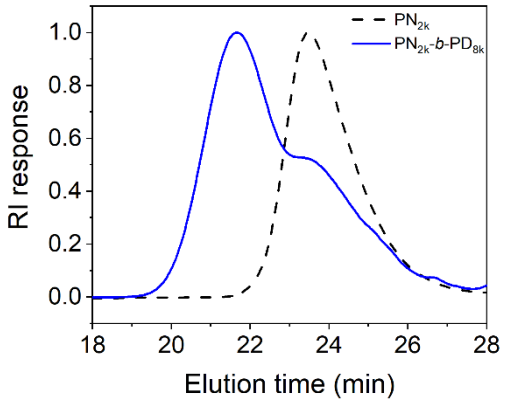

Figure S8. SEC traces of PN_2 and PN_{2k}-*b*-PD_{8k} in DMF (containing 10 mM LiBr).

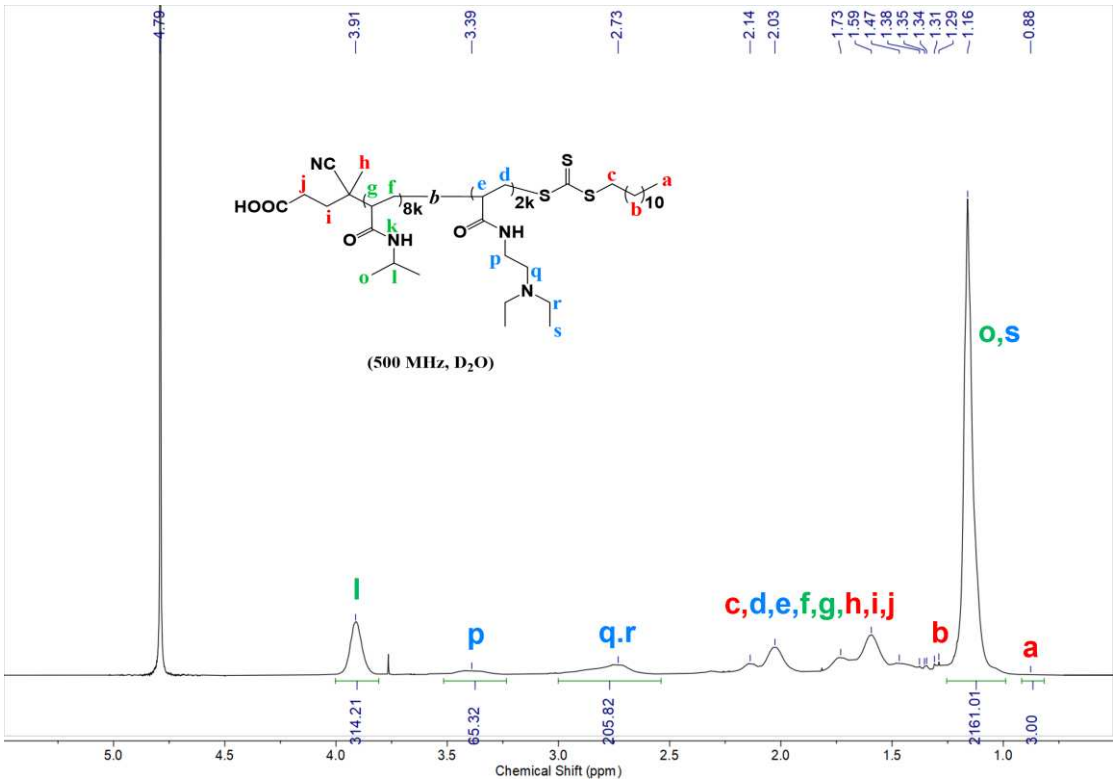

Figure S9. ^{1}H NMR spectrum of PN_{8k}-*b*-PD_{2k} in D_2O.

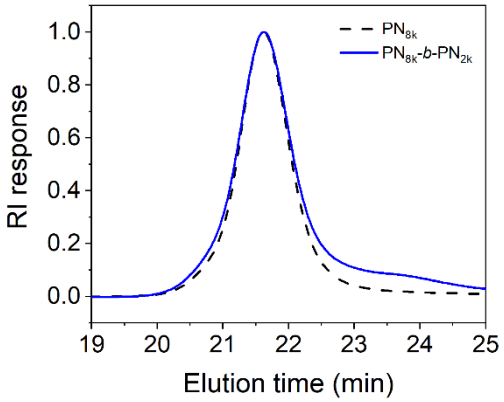

Figure S10. SEC traces of PN_{8k} and PN_{8k}-*b*-PD_{2k} in DMF (containing 10 mM LiBr).

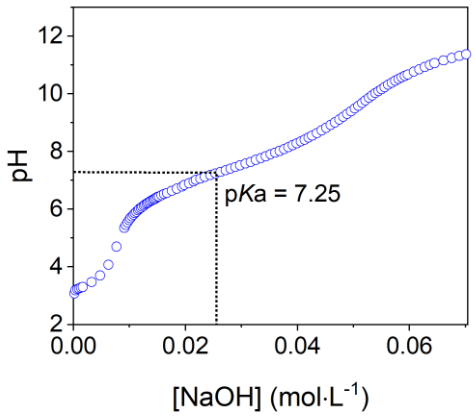

Figure S11. pH change of PD_{5k} homopolymer in water as a function of NaOH concentration.

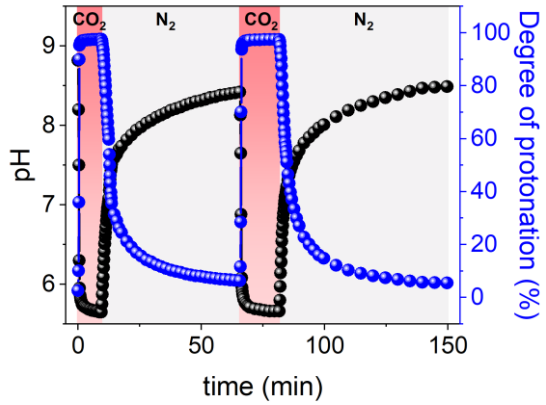

Figure S12. pH value and degree of protonation of PD_{5k} solution upon two cycles of alternately bubbling CO_2/N_2 ([PD_{5k}] = 0.1 wt.%, gas flow rate: 2 mL·min^{-1}).

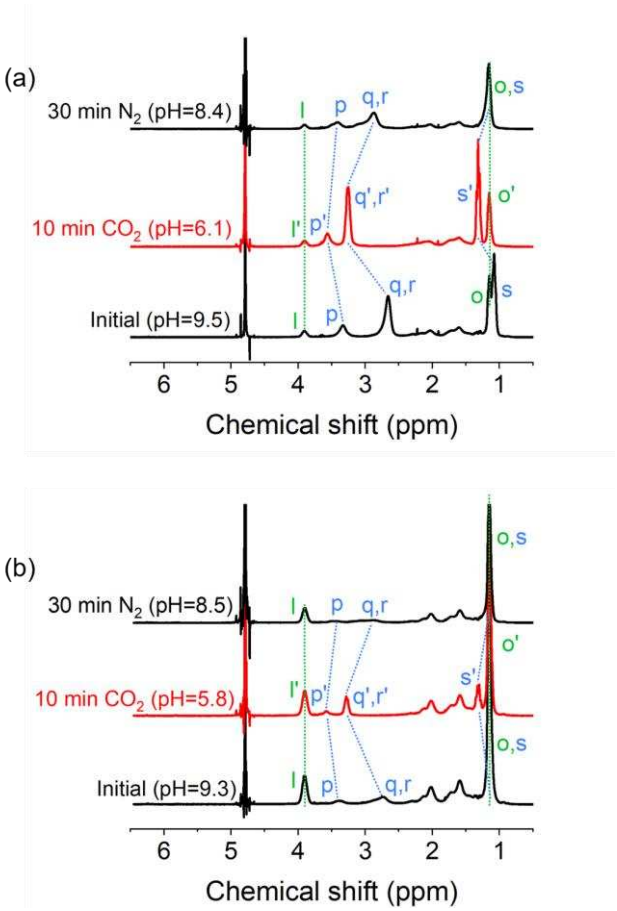

Figure S13. ^{1}H NMR spectra in D_2O of (a) PN_{2k}-*b*-PD_{8k} and (b) PN_{8k}-*b*-PD_{2k} recorded at 25 °C before and after exposure to CO_2 or N_2 ([PN-*b*-PD] = 1 wt.%, gas flow rate: 10 mL·min^{-1}, bubbling CO_2 and N_2 for 10 and 30 min, respectively).

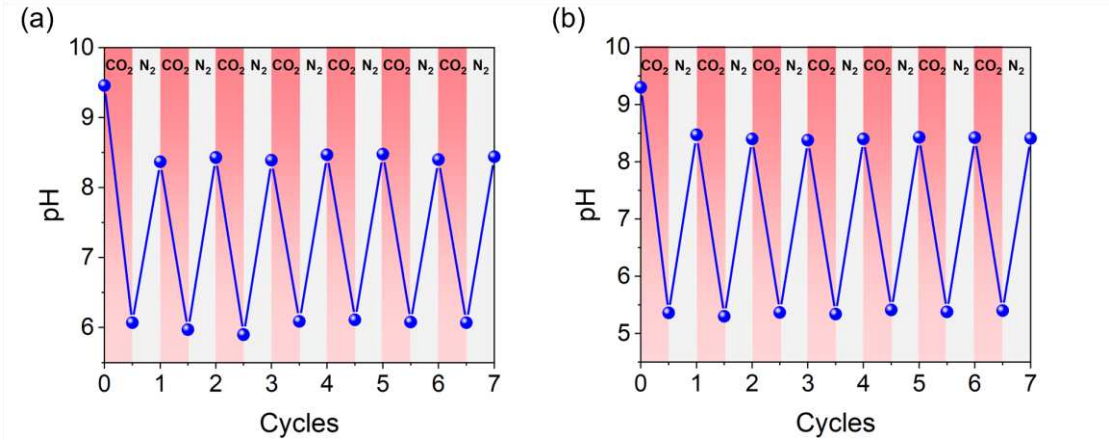

Figure S14. pH change of (a) PN_{2k}-*b*-PD_{8k} and (b) PN_{8k}-*b*-PD_{2k} systems measured at 25 °C upon seven cycles of alternately bubbling CO_2/N_2. ([PN-*b*-PD] = 1 wt.%, gas flow rate: 10 mL·min^{-1}, bubbling CO_2 and N_2 for 10 and 30 min, respectively)

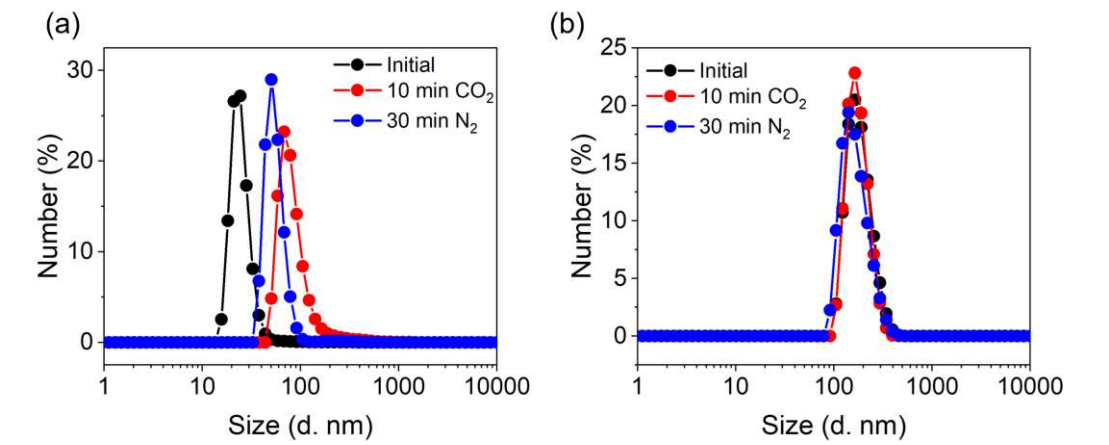

Figure S15. Number-averaged hydrodynamic size distribution of PN_{5k}-*b*-PD_{5k} before, after bubbling CO_2 and after bubbling N_2 (a) at 25 °C and (b) at 60 °C ([PN_{5k}-*b*-PD_{5k}] = 0.1 wt.%, gas flow rate: 10 mL·min^{-1}).

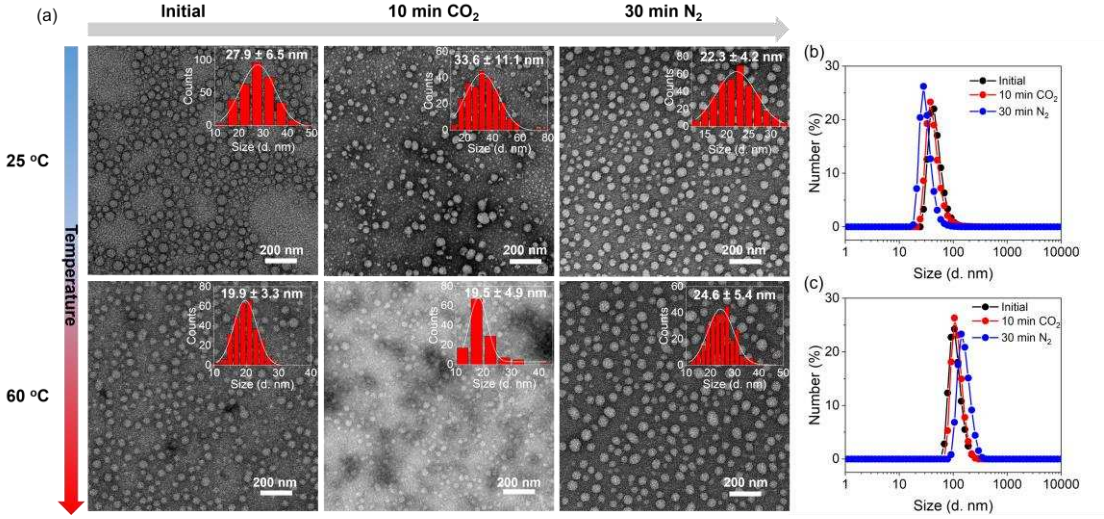

Figure S16. (a) TEM images of PN_{2k}-*b*-PD_{8k} aggregates formed before and after bubbling CO_2 or N_2 at different temperatures (25 and 60 °C). Number-averaged hydrodynamic size distribution of PN_{2k}-*b*-PD_{8k} before and after bubbling CO_2 or N_2 (b) at 25 °C and (c) at 60 °C. ([PN_{2k}-*b*-PD_{8k}] = 0.1 wt.%, gas flow rate: 10 mL·min^{-1})

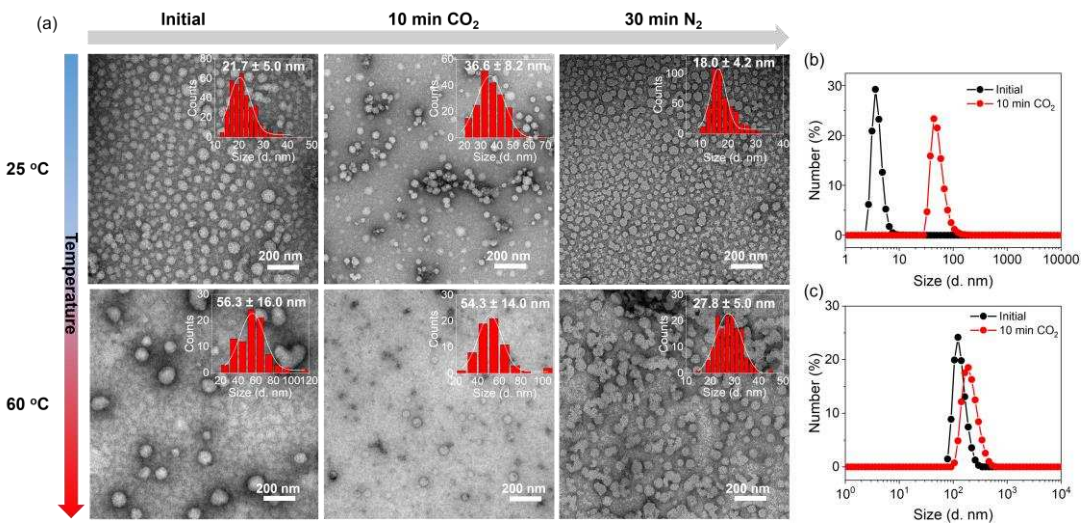

Figure S17. (a) TEM images of PN_{8k}-*b*-PD_{2k} aggregates formed before and after bubbling CO_2 or N_2 at different temperatures (25 and 60 °C). Number-averaged hydrodynamic size distribution of PN_{8k}-*b*-PD_{2k} before and after bubbling CO_2 or N_2 (b) at 25 °C and (c) at 60 °C. ([PN_{8k}-*b*-PD_{2k}] = 0.1 wt.%, gas flow rate: 10 mL·min^{-1})

References

[1] Z. Song, K. Wang, C. Gao, S. Wang, W. Zhang, Macromolecules 49 (2016) 162-171.

[2] F. Yin, P. Saint-Aguet, B. Lonetti, S. Gineste, Y. Coppel, N. Lauth-de Viguerie, J.-D. Marty, Submitted.